Journal of Hydrology 629 (2024) 130592

Contents lists available at ScienceDirect

Journal of Hydrology

journal homepage: www.elsevier.com/locate/jhydrol

Using multiple isotopes to determine groundwater source, age, and renewal rate in the Beishan preselected area for geological disposal of high-level radioactive waste in China

Jiebiao Li [a,b,c], You-Kuan Zhang [b,d], Zhichao Zhou [c,*], Yonghai Guo [c], Jingbo Zhao [c], Xiuyu Liang [b,*]

[a] School of Environment, Harbin Institute of Technology, Harbin 150090, China
[b] Guangdong Provincial Key Laboratory of Soil and Groundwater Pollution Control, School of Environmental Science and Engineering, Southern University of Science and Technology, Shenzhen 518055, China
[c] CAEA Innovation Center for Geological Disposal of High-Level Radioactive Waste, Beijing Research Institute of Uranium Geology, Beijing 100029, China
[d] Department of Earth and Environmental Sciences, University of Iowa, Iowa City, IA 52242

ARTICLE INFO

This manuscript was handled by Yuefei Huang, Editor-in-Chief

Keywords:
Multiple isotopes
Recharge source
Groundwater age
Renewal rate
High-level radioactive waste

ABSTRACT

Understanding hydrogeological conditions is crucial for selecting and assessing the long-term safety performance of a high-level radioactive waste (HLW) disposal repository. Utilizing environmental isotopes as effective markers for analysing groundwater movement, this study investigates groundwater recharge sources, age, and renewal rates using multiple isotopes in China's potential HLW repository site, the Beishan area. The results indicated deep bedrock groundwater primarily derives from ancient precipitation infiltration under cold climatic conditions. A noteworthy distinction is that loose sedimentary groundwater exhibits higher tritium content (>10 TU) compared to bedrock groundwater (<3.2 TU). Groundwater within the recharge area, especially within gullies and piedmont slope deposits, is relatively youthful, with an age of less than 30 years and an annual renewal rate exceeding 5 %. In contrast, the shallow groundwater age in the intermountain basins and depressions of the discharge area generally exceeds 50 years, with an annual renewal rate often falling below 0.5 %. At the Beishan underground research laboratory site, deep groundwater at the disposal repository depth displays a corrected ^{14}C age exceeding 8,000 years, indicating an extremely slow movement and alteration rate. As a result, the hydrogeological conditions in the Beishan area are expected to be relatively beneficial for ensuring the safety of HLW repository.

1. Introduction

High-level radioactive waste (HLW) is characterized by its extremely high levels of radioactivity, acute toxicity, long half-life, and heavy heat release. Safe and sustainable development of the nuclear energy industry depends on adequate management of HLW (Chapman and Hooper, 2012; Wang et al., 2006). At present, deep geological disposal is a feasible method of safely disposing HLW (Tsang et al., 2015). A comprehensive understanding of hydrogeological conditions is imperative for the site selection and safety assessment of HLW disposal repositories (Apted and Ahn, 2017; IAEA, 1989). To project the long-term performance of the repository, hydrogeological characteristics such as groundwater sources, age, and renewal rate must be resolved. The recharge, age, and renewal rate of groundwater reflect the comprehensive hydrogeological conditions of the area and can reliably reveal the movement and alteration of groundwater. These issues directly affect the migration of radioactive nuclides within the HLW repository and its long-term safety assessment.

To cast a forward-looking view on the enduring performance of repository, it is essential to dissect hydrogeological attributes encompassing groundwater sources, age dynamics, and renewal rates. Groundwater age, encapsulating the span between water entry into the groundwater system and the present, assumes a pivotal role in characterizing groundwater flow (Ferguson et al., 2020). Its widespread application extends to evaluating pathways of groundwater runoff, renewability, replenishment, and flow rates, often complemented by

* Corresponding authors.
E-mail addresses: zhouzhichao2006@163.com (Z. Zhou), liangxy@sustech.edu.cn (X. Liang).

https://doi.org/10.1016/j.jhydrol.2023.130592
Received 18 August 2023; Received in revised form 3 November 2023; Accepted 19 November 2023
Available online 6 December 2023

hydrogeological modeling (Ayraud et al., 2008; Kagabu et al., 2017; Zhang et al., 2021). On a parallel note, the groundwater renewal rate, derived from the annual recharge divided by the total reserve, emerges as a more objective metric, affording insights into the sustainable exploitation potential of groundwater resources (Ferguson et al., 2020).

The Beishan area is a priority area for China's HLW repositories, with widely distributed granite being essential to the repository structure. However, due to the pronounced spatial heterogeneity and anisotropy within the bedrock aquifer, along with limited observation data, the comprehensive understanding of groundwater distribution and circulation characteristics in the Beishan area, particularly pertaining to groundwater sources, spatial age distribution, and renewal rate, remains at a qualitative level. This limitation hampers the advancement of long-term safety assessments and the refinement of hydrogeological models.

Environmental tracers are well-recognized for providing valuable data on recharge sources, age, renewal rate, groundwater–surface water interactions, and mixing of groundwater masses (Batlle-Aguilar et al., 2017; Cartwright et al., 2017; Joshi et al., 2018; Kamtchueng et al., 2015; Ma et al., 2019). The isotope method uses the activity law of groundwater constituents at the atomic level to trace groundwater transport, providing an effective approach for analyzing groundwater movement in low-permeability bedrock such as the site of HLW disposal (Christofi et al., 2020; Cook et al., 2005; Priebe et al., 2021). It is the most effective technique for hydrogeological site selection for HLW disposal sites(Bockgård et al., 2004; Clauer et al., 1989; Gascoyne, 2004; Laaksoharju et al., 2008a).

The common environmental isotopes include, D, ^{18}O, ^{3}H, ^{14}C and noble gases isotopes. D and ^{18}O stable isotopes have been widely used for identifying groundwater recharge sources (Jasechko, 2019; Pang et al., 2017). Compared to modern groundwater recharge, the heavy isotope levels of paleo-meteoric groundwater recharge are typically lower (Pang et al., 2017; Zongyu et al., 2003). In addition, the stable isotopes of D and ^{18}O can be used to estimate the temperature of modern groundwater recharged by atmospheric precipitation (Barbieri et al., 2005; Jasechko, 2019; Siegenthaler and Oeschger, 1980).

The half-life of environmental radioactive isotope tritium (^{3}H) is 12.32 ± 0.02 years, which can distinguish between "old water" formed before 1953 and "young water" formed after 1953 (Jasechko, 2019; Lucas and Unterweger, 2000). As a constituent of water molecules, ^{3}H is unaffected by geochemical or biogeochemical processes occurring in soils and aquifers and has been demonstrated to be an indispensable tracer for accurately determining the groundwater age and renewal rate (Chatterjee et al., 2018; Cheng et al., 2021; Zhong et al., 2019). Owing to the influence of early nuclear tests and the latitudinal effect, ^{3}H activity in atmospheric precipitation in Northwest China remains high. Therefore, ^{3}H is the most used tracer for determining groundwater age in northwest China (Chen et al., 2006; Ma et al., 2019; Zhong et al., 2019). To rationally evaluate groundwater age according to hydrogeological conditions, tritium time-series data or multiple tracers can be used (Cartwright et al., 2017; Cheng et al., 2021; Liu et al., 2014).

Paleo-groundwater dating is crucial for determining groundwater residence times, deep groundwater circulation patterns, and associated dynamics for geological disposal sites of HLW (Nilsson et al., 2020). Carbon-14 (^{14}C) dating is widely used for determining the age of paleo-groundwater, especially in the selection of geological disposal sites for HLW, with optimal dating range 1–40 ka (Cartwright et al., 2017; Laaksoharju et al., 2008b). Previous studies have indicated that the deep bedrock groundwater age in the Beishan area is on the scale of ten thousand years, making it suitable to use the ^{14}C dating method (Zhou et al., 2022). Sweden, Finland, and Switzerland also have employed ^{14}C dating in their research on repository site selection and long-term safety performance assessment for geological disposal of HLW (Gimeno et al., 2023; Jr et al., 1991; Pitkaenen et al., 2004).

Noble gases exhibit negligible reactivity in hydrochemical processes, making their isotopes primary geochemical indicators for identifying gases derived from the Earth's mantle (Niu et al., 2017; Tian et al., 2021). Especially in bedrock areas, analyzing the rare gases in shallow and deep groundwater can effectively trace the cycling process of groundwater(Gumm et al., 2015; Tomonaga et al., 2017; Warr et al., 2018). The $^{3}He/^{4}He$ ratio (often denoted as R) enables the assessment of material proportions from Earth's crust and mantles, while the $^{4}Ne/^{20}Ne$ ratio identifies atmospheric influence on samples (Sano and Wakita, 1985).

The comprehensive utilization of multiple isotope analyses can help reduce uncertainties associated with the partial isotope method when interpreting hydrogeological issues, leading to more robust and reliable results (Clark and Fritz, 1997). This is particularly challenging in low-permeability bedrock areas with limited reserves and exhibit strong spatial heterogeneity, especially when collecting deep groundwater samples and interpreting the isotope data, which poses a significant challenge for isotope research (Guo et al., 2013; Zhou et al., 2020). To the best of our knowledge, there remains an unexplored realm where multiple isotopes are concurrently harnessed to delineate groundwater recharge, age, and renewal rate, particularly within the challenging context of low-permeability aquifers of the Beishan area. To address this gap, this study takes the Beishan area of the HLW repositories as an example to undertake a multi-isotope (D, ^{18}O, ^{3}H, ^{14}C and noble gases) study of groundwater circulation. This study aimed to offer a comprehensive depiction of the hydrogeological characteristics of the groundwater in the Beishan area. Moreover, this is the first time in China to research the multiple isotopes characteristics of the large-scale Gobi Desert, with particular emphasis on the following aspects: a) identifying the stable isotopic characteristics and recharge sources of groundwater based on stable isotope and noble gases isotope, b) characterising the spatial distribution of ^{3}H contents in groundwater, c) estimating the age of groundwater, and d) estimating the spatial distribution characteristics of shallow groundwater renewal rate.

2. Study area

The Beishan area occurs in a typical arid Gobi Desert, located north of the Hexi Corridor and west of the Heihe River Basin in Northwest China, with an area of more than 4×10^{4} km^{2}. The Beishan is a priority area for China's HLW repositories, the Xinchang site located in the Beishan area was chosen as China's first underground research laboratory (URL) site (Wang et al., 2018). Jiujing, Shazaoyuan, Yemaquan, and Suanjingzi are another four candidate sites in the preselected Beishan area (Fig. 1). The study area has a low mountain and hilly topography, with a relatively flat terrain overall. Surface conditions are typical of the Gobi Desert, with sparse vegetation and exposed bedrock. A few herders live scattered throughout the region, whereas others are temporary residents of mining enterprises. Annual precipitation is minimal, in contrast to evaporation rates, the atmosphere is dry and cold, and the sand is wind strewn. According to local meteorological data, the mean annual precipitation is $\sim$ 70 mm (Li et al., 2022). The average yearly temperature is about 8 °C, with a significant daily temperature difference. Generally, June through August are hot months with temperatures $>$ 30 °C. The wind direction is predominantly west and northwest. The study area has no perennial surface water; however, well-developed gullies formed by seasonal floods occur throughout the site (Guo et al., 2013). We extracted the distribution of the gully system in the Beishan area using a surface digital elevation model (Fig. 1c) and found that they are mainly distributed in an east–west direction.

The Beishan area is located on the northeastern margin of the Tarim block, which connects the Tarim, Sino-Korean, and Siberian blocks. There is a long geological evolutionary process and a complex orogenic belt structure. Regarding regional tectonic, the Beishan area is part of the Tarim Block (Li et al., 2020b), which exhibits a complex stratum, and the strata exposed from the Proterozoic to Quaternary are relatively complete (Yun et al., 2020). Groundwater can be categorized into four types, distinguished by the topography, landform, lithological structure, and geological structure: pore water in deposits, pore-fracture water in

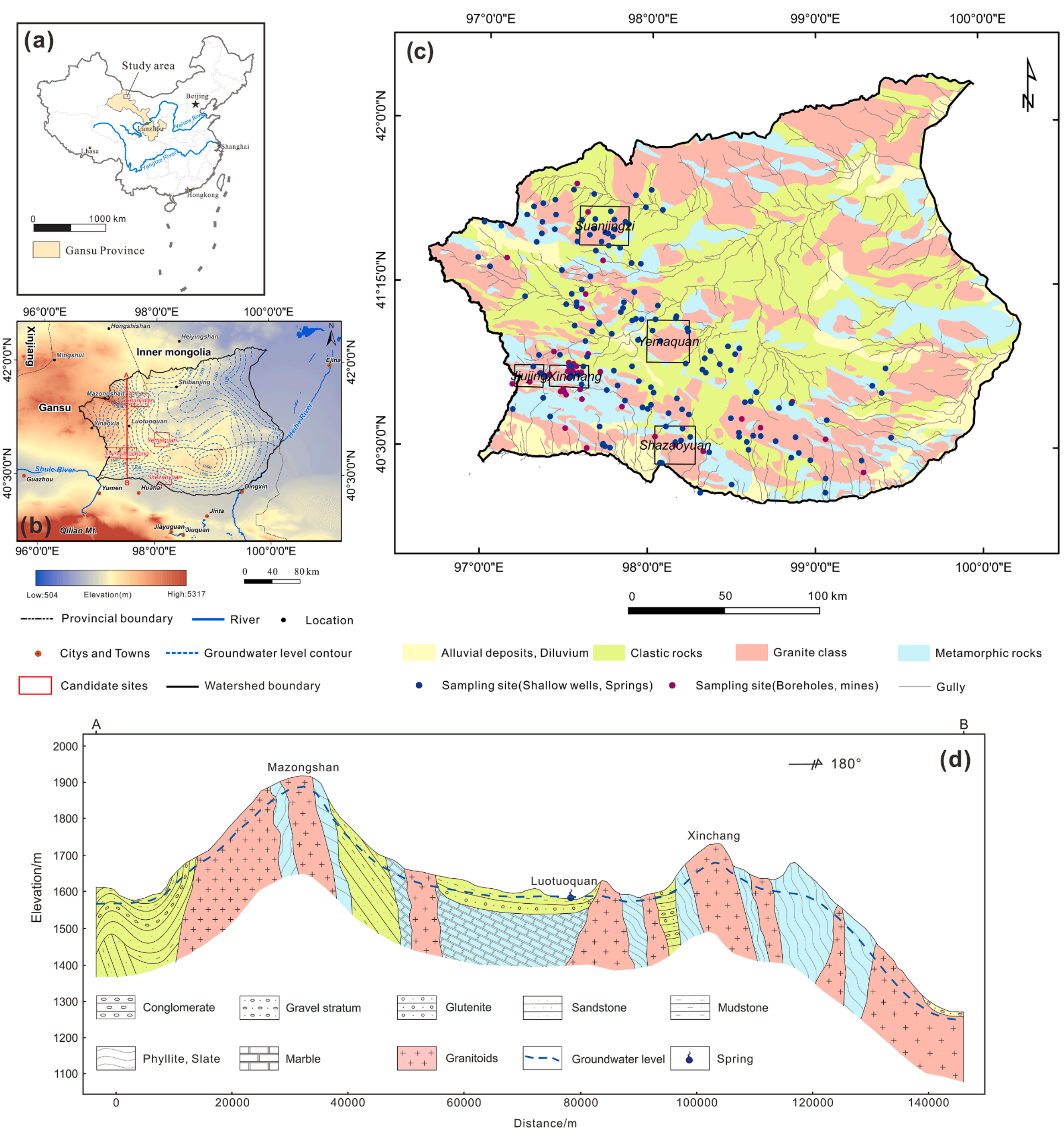

Fig. 1. (a) The location of the study area within China. (b) The contour maps of topography and groundwater level in the Beishan area. (c) Hydrogeological map in the Beishan area and sample locations.

clastic rocks, fissure water in metamorphic rocks, and fissure water in granite (Fig. 1c). The pore water in the deposits is mainly distributed in the gullies, intermountain depressions. The depth to groundwater level in the gully is mostly 1–3 m. Clastic rocks from different geological periods are widely distributed in hilly areas, mainly in the Cretaceous and Jurassic systems. The metamorphic rocks are primarily distributed in an NW–SE direction, while the water-bearing medium mostly comprises weathered and structural fractures. Mineral deposits are mainly distributed in the metamorphic rock areas. The groundwater level is generally 10–30 m, magmatic rocks are widely distributed, and the exposed area accounts for approximately 1/3 of the total bedrock area in Beishan. Terrain exerts a substantial influence on groundwater level. The groundwater level is generally < 5 m in low-lying areas, whereas the higher topography is mostly between 10 and 40 m. The primary direction of groundwater flow in the region is from west to east, with the main discharge area located in the downstream region of the Heihe River Basin. South of the Beishan area, the groundwater flows from north to south, and the Hexi Corridor is the local discharge area.

3. Date and methodology

3.1. Sample collection and analyses

Given the limited availability of sampling points in this area, which include shallow wells, springs, mines, and boreholes, our sampling approach aims to be as comprehensive as possible, with a primary emphasis on collecting water from mines and boreholes. For ^{14}C and gas isotope sampling points, the primary focus is at the Xinchang site and its surroundings. A total of 212 groundwater samples were collected from the Beishan area between 2014 and 2018. Among these, 160 samples were collected from shallow wells (mostly in the gully and piedmont slope loose deposits, where the groundwater level depth is generally between 2 and 5 m and the well depth is generally < 10 m) or springs. The remaining 52 samples were collected from boreholes or mines. Additionally, 97 precipitation samples (including 12 snowfall samples) were collected between 2012 and 2019. The pervious hydrogeological survey in the Beishan area revealed that the thickness of the weathering zone varies but generally ranges from several tens of meters to nearly 100 m, especially in proximity to fault zone (Fu et al., 2022; Guo et al., 2013; Zhou et al., 2022). Hence, to characterize the influence of the weathered zone on groundwater flow, this study classifies groundwater at depths greater than 100 m as deep groundwater and groundwater at depths less than 100 m as shallow groundwater. Most shallow wells and mines were used, and unused wells were pumped for more than half an hour before sampling to ensure the reliability of samples. A clean-water drilling scheme was adopted for all boreholes. Fluorescent sodium was added to the drilling fluid to obtain reliable groundwater samples. Sampling started when the concentration of fluorescent sodium tended toward zero, i.e., when the concentration of sodium fluorescein was < 1 % of the initial concentration. The double-packer system was used for sampling to obtain in-situ groundwater samples at different depths in the boreholes, especially for the deep groundwater samples, with a pumping time typically up to 1–3 months. In total, 23 groundwater samples were collected from boreholes, with the sampling depth > 100 m. All samples were placed into dry and clean HDPE plastic bottles, sealed with a sealing membrane, and stored at 4 °C until further analysis. To ensure the reliability of stable isotope analysis, a 0.45 μm filter membrane was used on-site to filter all water samples. Dissolved gas samples were obtained using on-site vacuum degassing technique. A comprehensive account of the techniques utilized for on-site acquiring dissolved noble gases in water can be found in the work by Lu et al. (2014). To ensure the quality of noble gas samples, minimizing the risk of gas loss and air contamination during the sampling process is essential.

All samples were analysed for ^{3}H and the stable isotopes of ^{18}O and D. A total of 31 samples of noble gases were analyzed. Among these, 15 samples were collected from shallow wells and springs (only 1 sample), 16 samples were collected from mines and boreholes (12 samples). A total of 23 samples were analyzed for ^{14}C dating, including. Noble gas and ^{14}C isotopic samplings are mainly concentrated near the Xinchang site (Fig. S1 and Fig. S2). The ^{3}H content of groundwater was analyzed using liquid scintillation spectrometry using ultra-low-level counters (Quantulus 1220, PerkinElmer, Waltham, MA, USA) at the Analytical Laboratory, Beijing Research Institute of Uranium Geology (Beijing, China). We used the alkaline cathode electrolytic concentration method, with a detection limit of 1.2 tritium units (TU) and an uncertainty level of < 1 TU. Before analysis, the samples were distilled and electrolytically enriched as previously described (Morgenstern and Taylor, 2009). TU was used to express ^{3}H content, and 1 TU corresponded to a $^{3}H/^{1}H$ ratio of 1×10^{-18}. The stable isotope ^{18}O and D levels were analyzed by a Finnigan MAT-253 stable isotope mass spectrometer (Thermo Fisher, USA, manufactured in Bremen, Germany), with reference to the Vienna standard mean ocean water (V-SMOW) standard. The analysis accuracies were 0.1 ‰ and 1.0 ‰, respectively. The ^{14}C content of groundwater was analyzed using an accelerated mass spectrometer (AMS) at the BETA laboratory in the United States, with a testing error of < 1 %. The isotope ratios of noble gases ($^{3}He/^{4}He$ and $^{4}He/^{20}Ne$) were analyzed by a noble gas mass spectrometer (Nu Instruments, UK) at the Key Laboratory of Petroleum Resources Research, Institute of Geology and Geophysics, Chinese Academy of Sciences. The instrument was calibrated using air samples collected from Gaolan Hill, located south of Lanzhou.

3.2. Reconstructing precipitation tritium contents

Tritium concentrations in groundwater are commonly correlated with atmospheric tritium fluxes to determine the groundwater age and renewal rate. It is essential to reconstruct the time series of precipitation tritium concentrations in the Beishan area to generate long-term observational data, which requires the tritium time series of precipitation from 1953 as precipitation input. Several methods can be used to reconstruct precipitation tritium time series, including the trend surface analysis method (TSAM) (Watson, 1971), Guan Bingjun method (GM) (Guan, 1986), double reference curve method (DRCM) (Doney et al., 1992), and triangular interpolation method (TM) (Celle-Jeanton et al., 2002), among others. Among these, TM and TSAM are interpolation techniques, whereas DRCM and GM are reference curve techniques. Table S1 shows the equations for each method, and Zhai et al. (Zhai et al., 2013) described the detailed algorithms.

Because the GM method considers the effects of nuclear tests in Northwest China, the GM method was used for the data from 1953 to 1971 (Guan, 1986). Monitoring data is available for the Xinchang site from 2012 to 2019. Four methods mentioned above were comprehensively examined to reconstruct the time series of ^{3}H contents in precipitation of the Beishan area from 1972 to 2011. For the interpolation method, the volume-weighted tritium data of Novosibirsk, Tashkent, Hong Kong, and Irkutsk from 1969 to 1983 were used for fitting. All methods were limited by the monitoring time of the precipitation tritium data. Accordingly, correlation equations were formulated to establish a relationship between the interpolated tritium concentrations in precipitation at the designated location and those observed in Ottawa during the reconstructed period. The Global Network of Isotopes in Precipitation (GNIP) monitoring data, especially from the Ottawa Station, revealed a drastic decrease in tritium concentration during precipitation in 1972 (Zhai et al., 2013). Because this sudden decline created uncertainty in the calculations, correlation equations were derived using the tritium time series during 1972–1983, and the tritium concentrations in the precipitation were extrapolated to other periods covering the Ottawa period, 1953–2019. The Nash–Sutcliffe model efficiency coefficient (NSE) was used to assess the quality of the simulation results (Gupta et al., 2009; Li and Si, 2018). The reconstructed results were compared with the measured data from 2012 to 2019 at the Xinchang site, and the method with the smallest NES was selected.

3.3. Groundwater age estimation

For the loose sedimentary groundwater, this study used the ^{3}H isotopic dating method. Regarding the bedrock groundwater, both ^{3}H and ^{14}C dating methods were used in this research. Groundwater age has been interpreted using several lumped-parameter models (LPMs) since the 1950s (Eriksson, 1971; Małoszewski and Zuber, 1982; Vogel, 1967). LPMs consider the groundwater system as a black-box model, neglecting the spatial heterogeneity of the parameters and characterizing the system with calibrated parameters. For a groundwater system that is in a steady-state, the tracer concentrations that are modeled at the outlet can be determined using a convolution integral (Małoszewski and Zuber, 1982):

$$C_{out}(t) = \int_0^{\infty} C_{in}(t-\tau)e^{-\lambda\tau}g(\tau)d\tau \tag{1}$$

where $C_{out}(t)$ and $C_{in}(t)$ are the output and input concentrations, respectively; t is the date of sample collection; τ is the date when a water parcel enters the system; λ is the radioactive decay constant; and $g(\tau)$ is the distribution function of transit time or exit age, which characterizes the flow of groundwater from a recharge area (inlet position) to an outlet position within the aquifer.

There are several LPMs available, such as FLOWPC (Maloszewski and Zuber, 1996), LUMPED, LUMPEDUS (Ozyurt and Bayari, 2003), TRACERMODEL (Böhlke, 2006), and TracerLPM (Jurgens et al., 2012). To address the problem of nonunique multiple solutions for tritium dating, we used TracerLPM (version 1.1.0). TracerLPM is an interactive

Excel workbook program developed by the USGS that is used to evaluate groundwater age (Jurgens et al., 2012). Using a custom search algorithm and solver, the best-fit solution is determined by minimising the total error between the measured and LPM tracer output concentrations. TracerLPM can also be used to accurately evaluate groundwater age using time-series data (Chatterjee et al., 2018).

PFM assumes a conservative tracer to follow a direct path from the recharge area to the sampling point without hydrodynamic dispersion or mixing. The PFM can be utilized for the analysis of both shallow unconfined, and confined aquifers, which are characterized by short-screened wells or a small recharge area (Jurgens et al., 2012). In this model, the function describing the exit age distribution is as follows:

$$g(\tau) = (\tau - \tau_m) \tag{2}$$

where δ is the Dirac delta function. The PFM can then be solved as:

$$C_{out}(t) = C_{in}(t - \tau_m)e^{-\lambda\tau_m}\ for\ t = \tau_m;\ 0\ for\ t \neq \tau_m \tag{3}$$

According to field hydrogeological investigations, the depths of shallow wells were typically < 10 m, with an extremely low amount of vertical infiltration recharge. The degree of dispersion or mixing was small, which conforms to the PFM assumption (Fig. S3). In addition, springs can be considered to conform to the piston flow. For boreholes and mines, the ^{3}H content of most groundwater samples was below the detection limit, and the groundwater age should be over 66 years (with the sampling date as the end-member date). The time-series mode in the TracerLPM program was used for sampling points in the time-series data.

Tritium and groundwater age results were mapped and interpolated to clarify the spatial distribution of shallow groundwater (i.e., phreatic water). Given the limitations of different interpolation methods, we used ordinary and empirical Bayesian kriging methods in this study. As the boreholes were mainly distributed near the Xinchang site, the tritium content in the groundwater samples collected from the boreholes was mostly below the detected value. However, the groundwater samples obtained from shallow wells exhibited a high tritium concentration. To reduce errors related to this data skew, borehole samples were excluded during the interpolation.

The principle of radiocarbon dating is the decay process of the radioactive carbon isotope. The apparent ^{14}C groundwater age assumes that all dissolved inorganic carbon (DIC) within groundwater derives from exchange reservoirs, such as the CO_2 in the soil. The equation is calculated as follows (Münnich, 1957):

$$\tau = \frac{5730}{\ln 2}\ln\left(\frac{^{14}C_0}{^{14}C_{DIC}}\right) \tag{4}$$

where τ is the groundwater apparent ^{14}C age, 5730 is the decay constant of ^{14}C, $^{14}C_0$ is the initial ^{14}C content of DIC ($^{14}C_0$ is typically set at the pre-nuclear test (1950 CE) atmospheric CO_2 level, which is approximately 100 pMC.), $^{14}C_{DIC}$ is the measured ^{14}C value of the DIC in the water sample.

Understanding the radiocarbon age of DIC in groundwater is challenged by uncertainties in predicting pre-nuclear-detonation ^{14}C levels during recharge and accounting for hydrochemical and physical processes that modify ^{14}C content along groundwater pathways. Therefore, the apparent groundwater age needs to be corrected to accurately reflect the average residence time of groundwater within the aquifer. Currently, several models have been proposed for correcting the apparent groundwater ages. Among these, the Pearson model, Han & Plummer model, IAEA model, and Oeschger model are accorded primary consideration (Han and Plummer, 2016). Nevertheless, the groundwater ages corrected by different models often yield varying results, and sometimes the errors can be significant. Considering the variations in geochemical processes among different models, the selection of an appropriate model should be based on the on-site hydrogeological conditions. In the study, the graphical method introduced by L.F. Han (2016) was used to facilitate relatively accurately determine the geochemical processes during groundwater flow. For detailed principles, please refer to the paper by Han and Plummer (2016).

Attention should be paid to the inherent limitations and uncertainties associated with each dating method. ^{3}H dating method is primarily suitable for relatively young groundwater, typically within the range of years to decades (Cartwright et al., 2017). Besides, accurately determining the ^{3}H input function of infiltrated water can be challenging due to spatial and temporal variations in ^{3}H concentration in precipitation and differences in hydrogeological conditions within the vadose zone. Decades after the bomb-pulse peak of atmospheric ^{3}H activity, the ^{3}H concentration in many regions has returned to or approached environmental background levels, limiting the use of ^{3}H dating methods. ^{14}C dating method is applicable to the ancient paleo-groundwater. However, it is difficult to accurately understand carbon sinks, carbon sources, and carbon behavior in the unsaturated zones (Han and Plummer, 2016). Additionally, it is challenging to identify all carbon sources and all reactions that affect carbon mass transfer. Furthermore, the mixing of young groundwater can also affect the accuracy of ^{14}C dating results.

3.4. Renewal rate estimation

The groundwater renewal rate, which reflects the characteristics of groundwater circulation, can be determined by calculating the annual recharge divided by the total reserve. We employed a well-mixed reservoir model and an equal-proportion mixing model, which are applicable to hydrological systems in arid regions. The well-mixed reservoir model assumes that groundwater originating from annual time-step recharge occurrences homogenizes entirely within the aquifer and that the aquifer is steady. The tritium concentration in groundwater was estimated by evaluating the radioactive decay of the solution and the annual inflow using the following approach (La Salle et al., 2001):

$$^3H_{gi} = \left(1 - R_i\right)^3H_{gi-1}e^{-\lambda} + R_i{}^3H_{0i} \tag{5}$$

where R denotes the annual renewal rate, unit is %; ^3H_g and $^3H_0$ are the ^{3}H activity of the groundwater and input water, respectively; λ is the radioactive decay constant for ^{3}H (0.05626 a^{-1}); and i is the time between 1953 and 2019.

The ^{3}H activity of the groundwater was calculated with a constant input activity ($^3H_0 = 10$ TU) by assuming a steady-state groundwater system before 1953 using the following equation:

$$^3H_{g1952} = \frac{^3H_0}{(\lambda/R + 1)} \tag{6}$$

The mixing model in equal proportions assumes that groundwater is vertically displaced within the aquifer by piston flow at a steady state. The groundwater recharged in different periods is stratified and only mixed during sampling. According to the mass balance principle, the equation is calculated as follows (La Salle et al., 2001):

$$^3H_{gw} = R\sum_{0}^{t_{max}} {}^3H_0\ e^{-\lambda t} \tag{7}$$

Where $^3H_{gw}$ is the tritium content in groundwater; $t_{max} = 1/R$ denotes the timing of the initial recharge event and the average annual renewal rate.

Before 1953, the groundwater system was assumed to be steady with constant input activity ($^3H_0 = 10$ TU), as in the previous model. The contribution of water infiltration before 1953 to groundwater activity was calculated as follows:

$$^3H_{gw1952} = R\frac{^3H_0\left(e^{-\lambda t_{67}} - e^{-\lambda t_{max}}\right)}{\lambda} \tag{8}$$

Where t_{67} represents the time interval from 1953 to the time of sampling, with most samples collected in 2019 (corresponding to the calendar years 1953–2019).

Generally, annual recharge is proportional to annual rainfall. The annual renewal rate (R_i) was weighted according to the mean renewal rate (R) and annual rainfall (P_i) and calculated as follows:

$$R_i = \frac{R(P_i - P_t)}{P_m - P_t} \tag{9}$$

Where P is the annual rainfall, P_m is the mean rainfall over several years, and P_i is the threshold rainfall. According to meteorological data from the Mazongshan and Yumen stations since 1953, the minimum rainfall was 24.6 mm. Thus 20 mm was selected as the approximate threshold.

Based on the different sampling times, the annual renewal rate calculated from the ^{3}H activity for both models was mapped. The estimated renewal rate only shows slight variations depending on the model chosen for the analysis (La Salle et al., 2001). Thus, only the model of a well-mixed reservoir was used for spatial analysis in this study. Empirical Bayesian kriging (EBK) and ordinary kriging (OK) methods were used, with borehole samples excluded during interpolation.

4. Results and discussion

4.1. Identification of groundwater recharge sources

(1)Stable isotope of D and ^{18}O

The global meteoric water line (GMWL) represents the long-term isotopic relationships between δD and δ^{18}O in global precipitation, with a slope of 8, attributed to the ratio of equilibrium fractionation factors (Craig, 1961). Variations in the slopes and intercepts of local meteoric water line (LMWL) and GMWL arise from differences in isotope fractionation in atmospheric precipitation under various climatic conditions (Jasechko, 2019). Therefore, to ensure the accurate interpretation of isotope data in groundwater within a specific region, it is essential to establish the LMWL (Putman et al., 2019). The LMWL in the Beishan area was established for the first time using the least square method and was calculated at δD = 7.53δ^{18}O + 4.28 (Fig. 2a). The amount-weighted precipitation δD and δ^{18}O values in the precipitation at the Xinchang site were –41.1 ‰ and –5.7 ‰, respectively. The slope and intercept of the LMWL are used to describe the origin and movement of water vapour and were more significant in the Beishan area than those in the Zhangye area. This indicates that the precipitation process in the Beishan area was less affected by secondary evaporation than that in the Zhangye area.

The composition of groundwater isotopes exhibited a dispersion phenomenon, especially in shallow wells (Fig. 2b). The average δD and δ^{18}O values for shallow wells were –56.0 ‰ and –7.3 ‰, respectively. The δD and δ^{18}O isotope values of groundwater collected in boreholes (deep groundwater) and shallow wells also showed significantly different. The average δD and δ^{18}O values for deep groundwater were –71.1 ‰ and –8.7 ‰, respectively. It can be found that groundwater δD and δ^{18}O values were lower than the amount-weighted precipitation. The difference may be mainly attributed to the recharge of shallow groundwater by precipitation that occurred under varying climate conditions (Jasechko, 2019). Over the past 50 years, the mean annual temperature in the area has risen by 1.39 ℃, exhibiting an average warming rate of 0.028 ℃/year (Zhou et al., 2022). Additionally, it's important to note that there is a significant elevation effect on isotopes in precipitation in the Beishan area (Li et al., 2020a). However, the majority of the precipitation samples in this study were collected around the Xinchang site, which might limit the representation of isotopic characteristics. Furthermore, there is also a significant elevation effect on groundwater isotopes in shallow wells (Fig. S4).

Groundwater from different sources may exhibit variations in δ^{2}H and δ^{18}O values along the LMWL. By comparing these distinctions, it becomes feasible to identify the groundwater recharge source and determine various parameters such as elevation, latitude, and temperature of the recharge area (Jasechko, 2019). The samples generally fell along or on the lower right of the LMWL (Fig. 2b), indicating that groundwater is sourced from local precipitation infiltration. Samples distributed along the LMWL were primarily collected in gullies with quicker groundwater circulation, which were less affected by evaporation. The samples distributed on the lower right side of the LMWL were mainly from the local discharge area and were enriched in heavy isotopes owing to evaporation. For shallow wells with tritium concentrations > 10 TU, the slope of the evaporation line was approximately 5.4. According to the correlation between δ^{18}O and the mean monthly surface air temperature in northwest China, δ^{18}O = 0.31 T(°C) – 12.69 ‰ (Guo et al., 2015), the mean surface air temperature of atmospheric precipitation recharge for shallow wells was ~ 17.4 °C, which was consistent with the average temperature during summer in the Beishan area. Furthermore, precipitation in the Beishan area is concentrated from June to August, constituting more than 60 % of the annual total, and is characterized by heavy rainfall. In contrast, winter snowfall accounts for less than 10 % of the annual precipitation. In summary, the primary source of shallow groundwater in the Beishan area is local precipitation infiltration, significantly influenced by the heavy summer rainfall during the recharge year.

The deep groundwater samples were located more towards the lower right of the LMWL compared to the shallow groundwater samples. Precipitation recharge from ancient paleo-meteoric recharge during cooler climates can explain the depletion of isotopes in groundwater (Clark and Fritz, 1997; Zongyu et al., 2003). Studies have shown that the apparent age of deep groundwater ^{14}C is generally > 8 ka, corresponding geological age is mainly the early Holocene and late

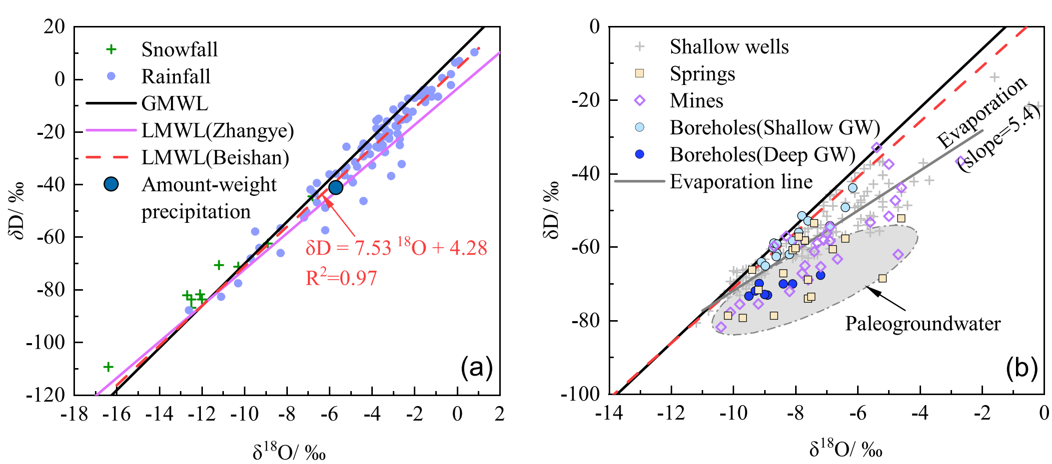

Fig. 2. Distribution characteristics of the stable isotope δD and δ^{18}O (a) LMWL in the Beishan area. (b) δD and δ^{18}O levels in the groundwater samples.

Pleistocene (Guo et al., 2013; Zhou et al., 2022). During this period, the atmospheric temperature was significantly lower than in the current era, and a notable cooling event called the 8.2 ka event occurred (He et al., 2012; Wurster et al., 2008). Therefore, the observed variation in the isotopic composition of deep bedrock groundwater may be attributed to recharge that occurred under colder climate conditions. In addition, some mine and spring groundwater samples (shadow range in Fig. 2b) were similar and fell near the deep groundwater samples. Furthermore, the tritium concentration of these springs was below the detection limit. Hence, we speculated that these samples were also primarily recharged by the infiltration of ancient atmospheric precipitation.

(2)Noble gas isotope

As shown in Fig. 3, three distinct endmembers with unique helium and neon isotopic compositions exhibit specific ratios, reflecting atmospheric, crustal, and mantle components: atmospheric ($R/R_A = 1$, $^4Ne/^{20}Ne = 0.318$), crustal ($R/R_A = 0.025$, $^4Ne/^{20}Ne = 1000$), and mantle ($R/R_A = 8$, $^4Ne/^{20}Ne = 1000$). The interaction among these endmembers demonstrates mixing relationships. The main source of helium in groundwater from loose sediment (collected in shallow wells) and shallow bedrock (collected in mines and shallow boreholes) within the region is atmospheric. In deep bedrock groundwater, the primary sources of helium are atmospheric origin and stable crustal radioactive decay and helium isotopes do not exhibit characteristics indicating a deep mantle origin. This further illustrates that deep groundwater originates from local precipitation recharge and has not undergone deep cycling processes. Furthermore, the helium isotopes in samples collected from the spring located in Houhongquan also derive from precipitation and in-situ radioactive decay, indicating a relatively old groundwater age. Field hydrological investigations have revealed that the spring is an artesian spring with a long flow path.

4.2. Tritium content in groundwater

Generally, the amount of tritium in groundwater is directly related to the residence time. The tritium content of shallow well groundwater was between 1.2 TU and 59.54 TU, mostly > 10 TU (Fig. 4), which indicates brief residence times for groundwater in loose sedimentary circulation. The samples with tritium content < 5.0 TU were mainly distributed in intermountain basins and depressions, especially the samples collected in the discharge area; the runoff conditions were poor, with high conductivity, and evaporation was apparent. The springs were primarily distributed near the middle local discharge area of Yinaoxia–Luotuoquan and the southern discharge area, and the tritium content of most samples was lower than the detection limit. The samples collected from mines and boreholes also showed low tritium contents (mostly < 3.2 TU), indicating poor circulation of the bedrock groundwater.

Based on the above analysis, tritium content varied significantly between the bedrock and loose sedimentary groundwater. The samples collected from both water-bearing media followed a log-normal distribution (Fig. 5a). The average tritium content in loose sediment was ~ 9.68 TU, whereas that in bedrock groundwater was ~ 3.12 TU. We analysed ^3H content variation with depth to determine its vertical distribution (Fig. 5b). ^3H content showed a dispersed distribution in loose sedimentary groundwater, with little regularity. The bedrock groundwater level was generally > 10 m, which is much deeper than that of loose rock groundwater. Over 70 m, the ^3H content was below the detection limit, further indicating that the proportion of modern water in the deep-bedrock groundwater was very small.

4.3. Groundwater age estimation

The monitoring results indicated that the tritium content of precipitation in the Beishan area was 12.5–47.5 TU between 2012 and 2019. The average tritium content of the rainfall samples was 30.03 TU, whereas that of the snow samples was 23.23 TU. No significant difference was found in the distribution of tritium content in atmospheric precipitation between locations during the same period. A direct comparison between the observed and reconstructed values showed that the TM method performed better than the other methods (Table S2 and Fig. S5), which is consistent with an assessment of China's Loess Plateau (Li and Si, 2018). From 1972 to 1983, the TM method was used to reconstruct the ^3H content of precipitation. Moreover, ^3H content was reconstructed using the correlation equation with Ottawa precipitation for 1984–2011 and monitoring data from the Xinchang site for 2012–2019. The reconstructed time series of tritium content in the

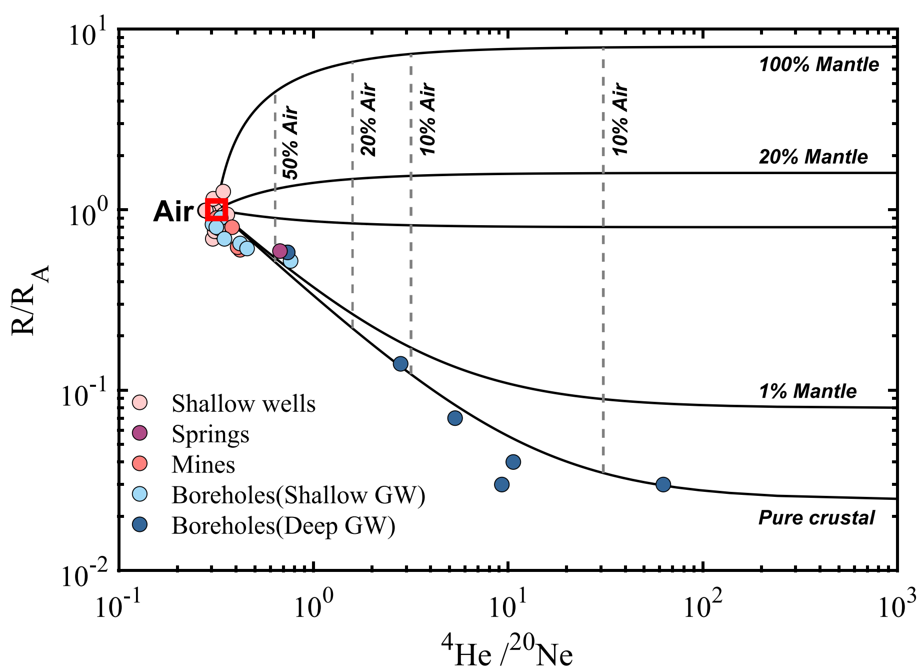

Fig. 3. Correlation diagram between $^3He/^4He$ and $^4He/^{20}Ne$ ratios of the groundwater samples in Beishan area. The mixing-boundary lines adhere to (Sano and Wakita, 1985).

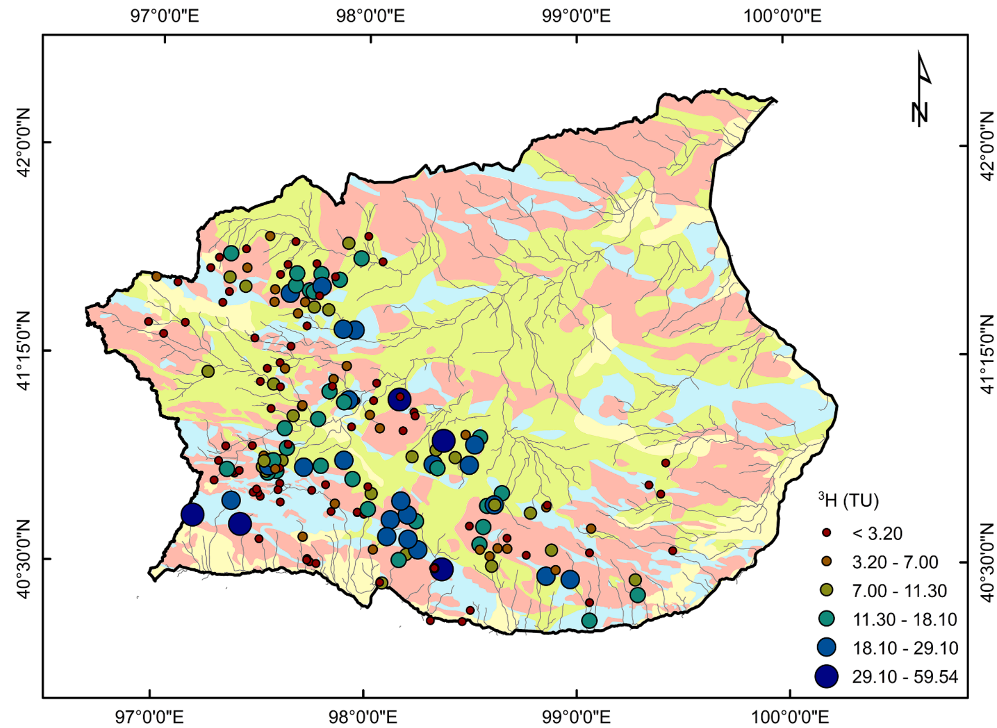

Fig. 4. Spatial distribution of tritium levels in the shallow groundwater of the Beishan area.

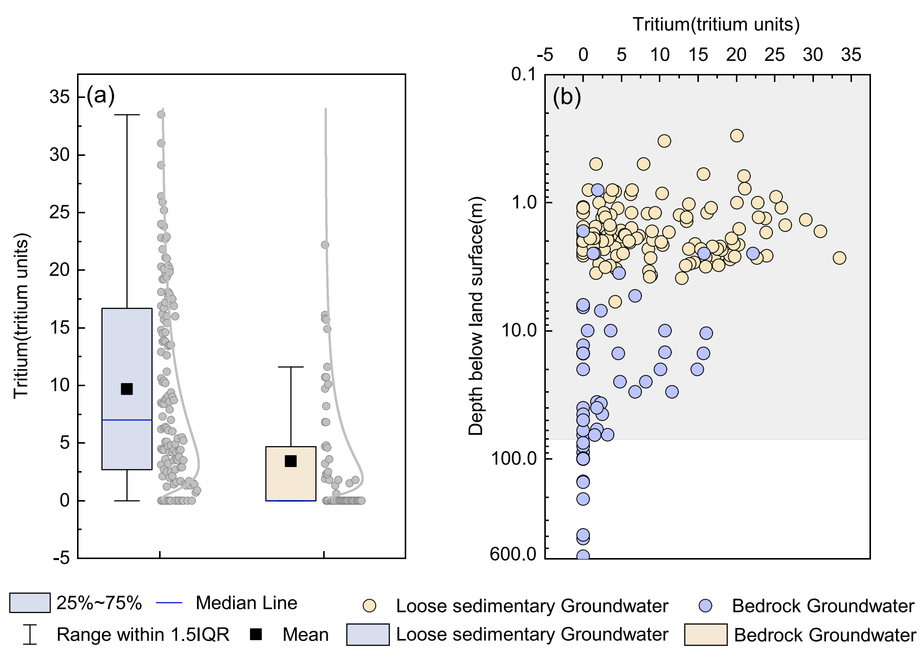

Fig. 5. Groundwater ^{3}H content (a) statistics for different water-bearing media and (b) variation with depth.

precipitation is shown in Fig. 6.

The shallow groundwater age was estimated using the PFM method based on the reconstructed atmospheric tritium time series in precipitation. Subsequently, two spatial interpolation methods were conducted, and the results are depicted in Fig. 7. We observed a slight difference between the results of the EBK and OK methods. This difference was mainly observed near Yinaoxia in the western part of the study area, possibly because there were fewer wells. The spatial distribution of groundwater age was strongly correlated with the groundwater flow path, and the groundwater age in the local recharge area was significantly younger than that in the local discharge area. The groundwater age is influenced by a variety of complex factors, including hydrogeological structure, hydraulic gradient, and aquifer permeability, among others. There are two apparent high-value groundwater age zones: the Yinaoxia–Luotuoquan area near the middle runoff area and the southern discharge area near the Huahai Basin. The groundwater age of the local recharge area was young, generally < 30 years, and mainly distributed in the gullies and piedmont slope deposits near the Xinchang, Suanjingzi, and Shazaoyuan sites. The gully was extensively developed in the study area, and Quaternary sand gravel alluvium of different

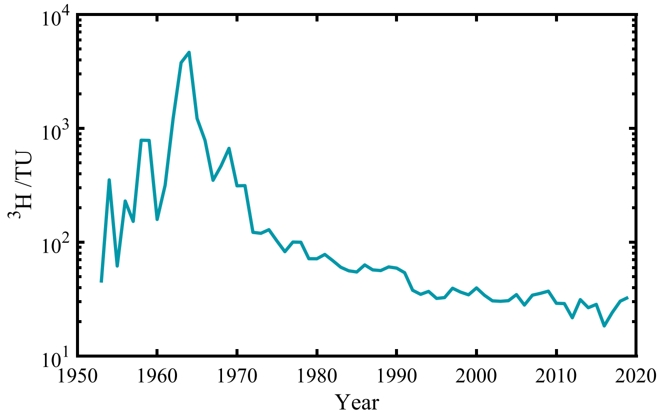

Fig. 6. Reconstructed time series of ^{3}H contents in precipitation of the Beishan area for 1953–2019.

thicknesses (generally < 10 m) was scattered over the top half of the gully depression. Runoff conditions were good and allowed for adequate infiltration recharge from precipitation, especially in the recharge area. The age of the bedrock groundwater on both sides was generally > 1 ka (Zhou et al., 2020), indicating a slow runoff process. Intermountain basins and depressions are widely distributed throughout the area. Sandstone, conglomerate, sandy mudstone, and interbedded mudstone are the primary terrestrial clastic rocks of Upper Cretaceous and Neogene deposits in these basins. The basin frequently acts as a local discharge region because of its weak runoff, lengthy flow paths, and high concentration of dissolved salts. The groundwater age of shallow groundwater in intermountain basins and depressions was typically > 50 years. The shallow groundwater age in the southern discharge area was also old.

At the Xinchang site, the groundwater flow directions were mainly southeast and northeast. The mean flow velocity of shallow groundwater was roughly estimated from the change in groundwater age along the flow path (Fig. S6), which was approximately 1.07 and 0.52 km/a for flow paths I-I' and II-II', respectively. The average hydraulic gradients were about 10.95 ‰ and 6.06 ‰ for flow paths I-I' and II-II', respectively. Based on Darcy's law, we speculated that there was little difference in the permeability of the phreatic aquifers between the two flow paths.

As shown in Fig. 5, most samples collected from mines and boreholes exhibited low tritium levels (< 3.2 TU), suggesting limited circulation of the bedrock groundwater. Especially for bedrock groundwater at depths over 70 m, the ^{3}H content was below the detection limit, so the tritium dating is no more appropriate. To determine the bedrock groundwater age, ^{14}C dating was used in this study. The sampling depths and the ^{14}C analysis results are presented in Table S3. The model selection diagram for bedrock groundwater in the study area is illustrated in Fig. 8, and the corrected results for groundwater age are shown in Table 1. Han and Plummer's graphical method classifies groundwater into three distinct groups.

The first group is mainly plotted within the zero-age zone and shows relatively high ^{14}C activities (52–80 pMC). Collected from shallow bedrock groundwater, most of these samples come from boreholes near a gully. The bedrock groundwater maintains a tight hydraulic connection with loose sedimentary groundwater within the gully. Applying the IAEA model for computations reveals that most of the corrected ages for these samples are < 3 ka. For certain boreholes, the corrected ages are close to or below the applicable lower limit (1 ka), and even has negative values. Therefore, to accurately determine groundwater age, alternative dating methods such as ^{39}Ar and ^{32}Si dating can be used (Lu et al., 2014). Furthermore, detecting slight tritium in certain samples (BS12 and BSQ25) indicates the mixing of modern water in the shallow bedrock groundwater of these boreholes. Most group (2) samples are in the Eichinger area, with some in the Mook area near the boundaries of both,

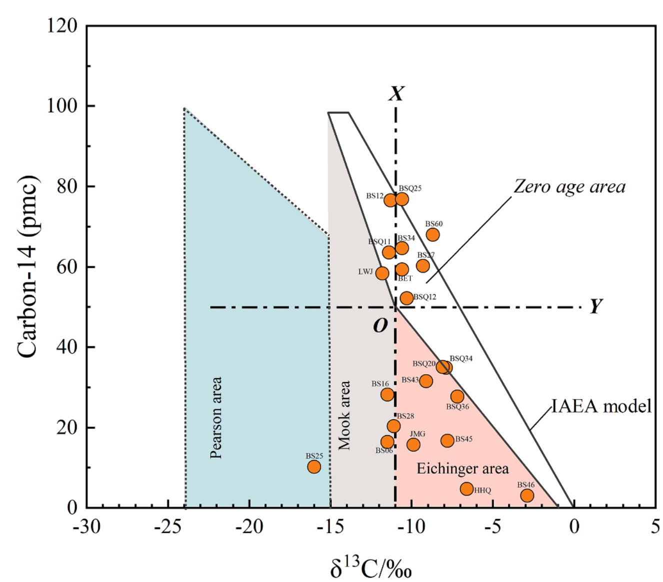

Fig. 8. Diagram for selecting groundwater age correction model (Underlying map from (Han and Plummer, 2016)).

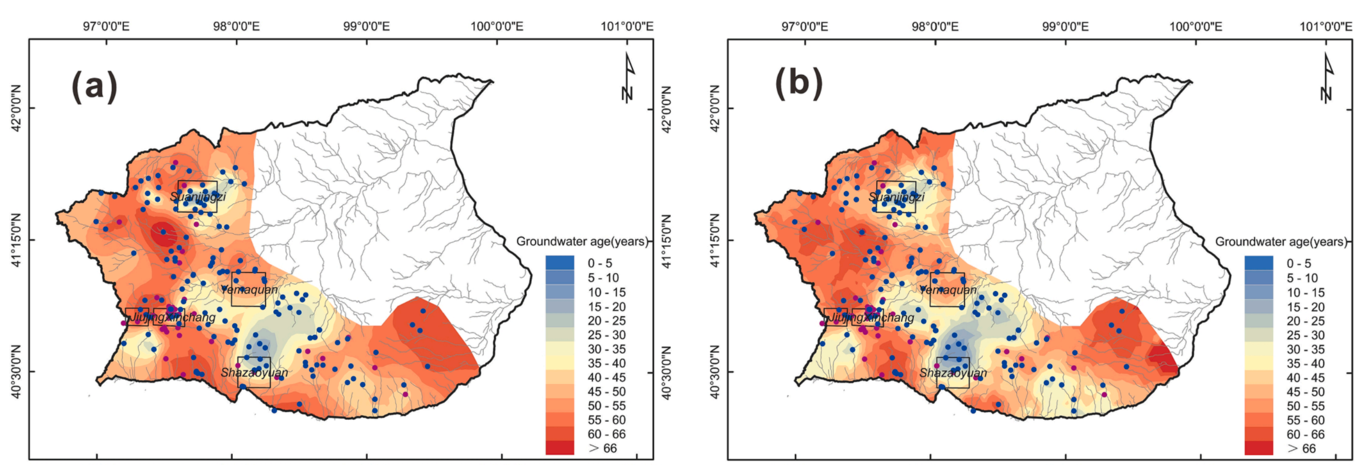

Fig. 7. Spatial distribution of shallow groundwater age in the Beishan area using the (a) EBK or (b) OK method.

Table 1
Correction results of bedrock groundwater ^{14}C age.

Sample ID	Uncorrected	Tamers model	Pearson model	Mook model	Eichinger model	IAEA model	Selected model
BS46	28.99	23.43	13.60	/	**17.44**	16.23	Eichinger
BS25	18.87	13.23	**15.99**	21.07	15.23	15.59	Pearson
BS28	13.18	7.57	7.45	6.58	**8.32**	11.17	Eichinger
BS60	3.19	−2.04	−4.57	/	−2.88	−0.62	/
LWJ	4.45	−0.97	−0.81	−0.77	−0.36	**3.32**	IAEA
BET	4.31	−1.16	−1.78	−1.85	−0.98	**2.37**	IAEA
BS34	3.60	−1.88	−2.49	−8.94	−1.66	**1.61**	IAEA
BSQ11	3.74	−1.61	−1.78	−3.30	−1.19	**2.38**	IAEA
BSQ12	5.37	0.16	−0.93	−5.32	1.69	**3.17**	IAEA
BSQ36	10.60	5.39	1.59	/	**4.01**	5.13	Eichinger
BS16	10.48	5.03	5.02	3.88	5.49	9.25	Mook
JMG	15.31	10.56	8.70	/	**10.15**	9.25	Eichinger
HHQ	25.26	20.15	15.60	/	**17.96**	19.53	Eichinger
BS45	14.81	9.63	6.40	/	**8.33**	10.39	Eichinger
BS06	14.94	9.53	9.48	**8.35**	9.98	13.70	Mook
BSQ34	8.70	3.40	0.38	/	**2.23**	4.38	Eichinger
BSQ20	8.67	3.34	0.47	/	**2.18**	4.70	Eichinger
BS12	2.21	−3.06	−3.38	−5.51	−2.77	**0.86**	IAEA
BS27	4.19	−1.14	−2.90	/	−1.53	**1.15**	IAEA
BSQ25	2.18	−3.28	−3.91	/	−3.14	**0.31**	IAEA
BS43	9.55	4.14	2.30	/	**3.83**	6.12	Eichinger

The table shows groundwater ages in units of ka, and"/" stands for no data.

which is typical for old waters (Han et al., 2012). These samples were mainly collected from deep bedrock groundwater within granite formations or shallow bedrock groundwater within metamorphic rock strata. The third group is only BS25, falling within the Pearson area, and belongs to the deep bedrock groundwater.

Overall, the corrected ^{14}C ages of shallow bedrock groundwater in the Xinchang site vary widely, ranging from 0.31 to 8.35 ka. The shallow groundwater ages of boreholes BS43 and BS45, located in metamorphic rocks, are considerably older than those of other boreholes in granite geology. This is easily understandable, as metamorphic rocks exhibit lower permeability. The corrected ^{14}C ages of deep bedrock groundwater is generally > 10 ka, indicating the groundwater movement and alteration were extremely slow. Moreover, the corrected ^{14}C age of the samples collected from the spring located in Houhongquan within the local discharge area is as high as 17.96 ka. Since the spring is mainly recharged by fractured bedrock groundwater from the western and southern mountainous regions, with the western recharge flow path about 20 km, and the depth of groundwater circulation ranges from about 200 to 300 m. It is worth mentioning that the corrected models neglect the influences of groundwater flow patterns and mixing, and thus the calibrated results might underestimate the realistic groundwater ages (Han and Plummer, 2016). The corrected ^{14}C ages collected from the depth interval of 355–484 m within borehole BS28 in the Beishan URL site is about 8.32 ka. Hence, it is speculated that the realistic age of the deep bedrock groundwater at the disposal repository depth (500–1000 m) within the URL site (> 300 m) should > 8 ka.

4.4. Estimation of groundwater renewal rate

Using the year 2019 as the sampling reference, we have depicted the relationship between groundwater annual renewal rates and tritium content in Fig. 9a. In the loose sediment, the average groundwater ^{3}H content was close to 10 TU, with an annual renewal rate of approximately 1 %. Conversely, in gully and piedmont slope deposits, the average ^{3}H content was approximately 16.82 TU, and the annual renewal rate reached around 4 %. However, groundwater annual renewal rates were notably low in the intermountain basins and depressions, often falling below 0.5 %. Additionally, the majority of bedrock groundwater and spring samples exhibited annual renewal rates of less than 1 %. As indicated by the probability distribution, the annual renewal rate of shallow groundwater was generally slow, with less than 10 % of the wells exceeding 10 % renewal, as shown in Fig. 9b.

In the Beishan area, the EBK and OK methods yielded slightly different results, as displayed in Fig. 10. The spatial distribution of

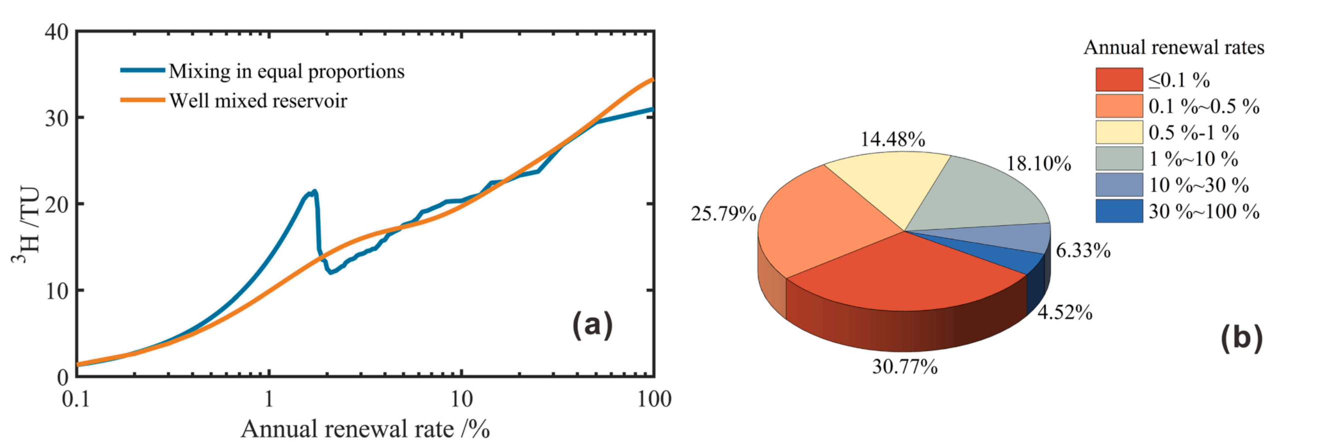

Fig. 9. (a) Annual renewal rate calculated from the ^{3}H content using both models for well-mixed reservoirs and mixing in equal proportions in 2019. (b) Probability distribution map.

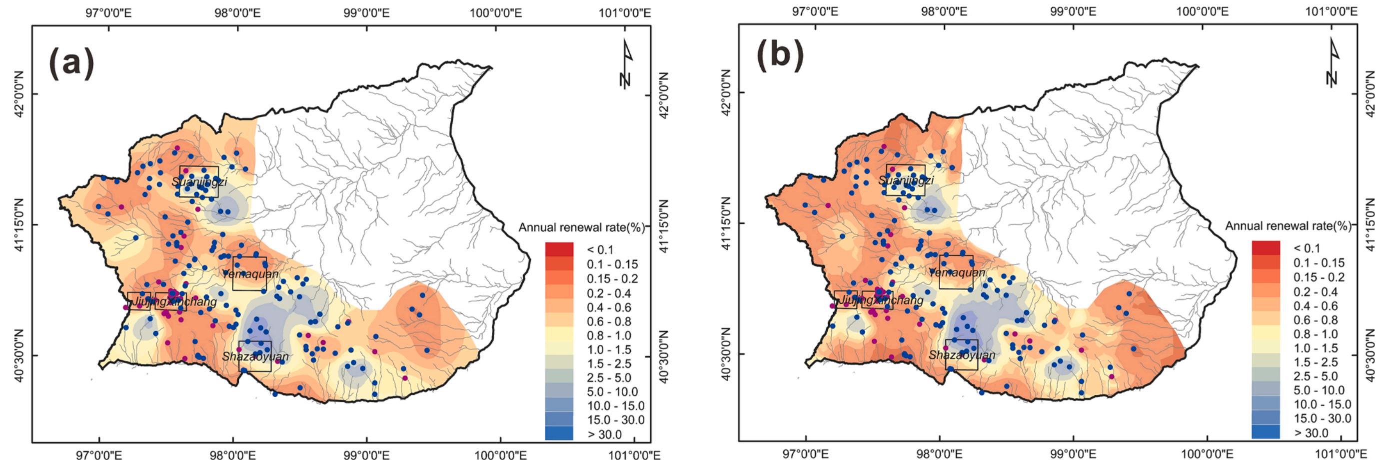

Fig. 10. Spatial distribution of shallow groundwater renewal rates in the Beishan area according to the (a) EBK and (b) OK method.

groundwater age and annual renewal rate generally exhibited alignment. Shallow groundwater in gully and piedmont slope loose deposits had relatively rapid annual renewal rates, often exceeding 1.5 % and reaching over 5 % at the Suanjingzi and Shazaoyuan sites. However, these deposits typically had a shallow depth of less than 5 m and modest well yields of less than 10 m^3/d (Guo et al., 2013). Groundwater yields in intermountain basins and depressions varied widely, influenced by basin size, lithology, and fault development. Shallow groundwater in intermountain basins and depressions typically experienced annual renewal rates ranging from 0.5 % to 1.5 %. Furthermore, the shallow groundwater annual renewal rate of most bedrock groundwater was exceptionally low. In summary, the exploitation potential of groundwater resources in the Beishan area is extremely limited.

4.5. Groundwater flow pattern

Based on the digital surface model and regional shallow bedrock groundwater contour map, it is evident that the Mazongshan–Suanjingzi is the regional recharge area (Fig. 11). The terrain slope in the Mazongshan Suojingzi area was relatively steep, with an average hydraulic gradient of approximately 12.6 ‰. As a result of the elevation effect, the average δD and $\delta^{18}O$ values of groundwater in the gully and piedmont slope loose deposits were found to be lower than those of the local recharge and discharge areas in the loose sediments. Besides, the

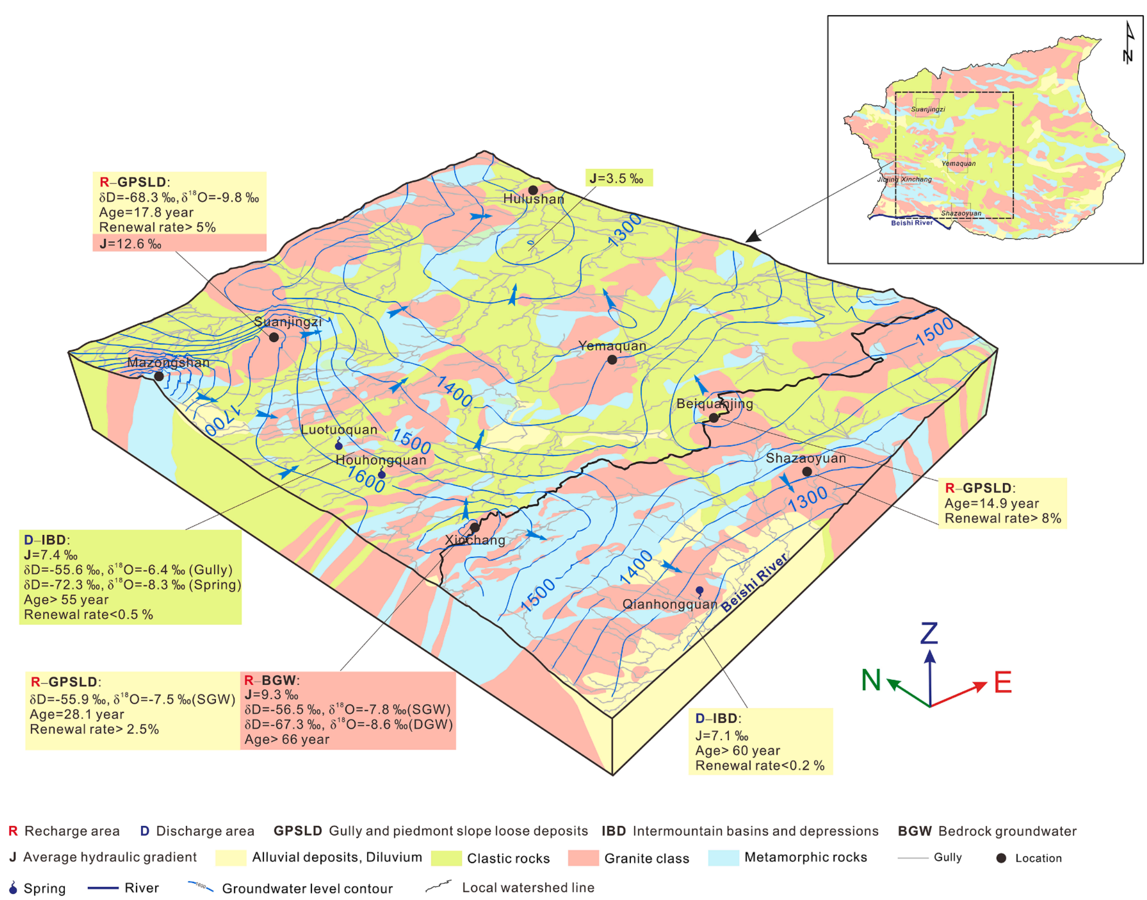

Fig. 11. Schematic diagram of the shallow groundwater flow pattern in the Beishan area.

mean groundwater age in the gully and piedmont slope loose deposits was estimated to be about 17.8 years, indicating rapid circulation and renewal.

Xinchang–Beiquanjing was situated within the local recharge area. Groundwater in the gully and piedmont slope loose deposits has a mean age of $<$ 30 years and an annual renewal rate of $>$ 2.5 %. At the Xinchang site, the groundwater age in the bedrock was significantly older than that in the loose sediments. Field surveys indicate that the groundwater level in the gullies was consistently higher than that in the adjacent bedrock areas on both sides. Consequently, driven by the groundwater head difference, the groundwater in the valley flows laterally to bedrock areas with high terrain on both sides (Fig. S7). Moreover, the average hydraulic gradient of bedrock groundwater at the Xinchang site was approximately 9.3 ‰.

The vicinity surrounding Luotuoquan–Houhongquan was the local discharge area, and the spring water is mostly exposed to the surface in the form of artesian springs. While the southern Beishi river area was classified as a regional discharge zone. The average hydraulic gradient in this area was relatively low, particularly in the Hulushan area, where it was only 3.5 ‰. Groundwater in these areas was characterized by its old age, and the annual renewal rate was extremely low, suggesting slow groundwater movement and alteration.

Finally, the groundwater flow pattern indicates that groundwater flow was primarily influenced by a complex interplay of various factors related to groundwater recharge, runoff, and discharge conditions. In the recharge area, the loose sedimentary groundwater exhibits a younger age and a higher annual renewal rate, while the aquifer thickness is thin and localized. Similarly, the shallow groundwater age and renewal rate were also low in the discharge area. Moreover, the movement and alteration of deep bedrock groundwater were characterized by an extremely slow rate.

The groundwater flow pattern is essential for determining the location of a HLW geological disposal site. Prioritizing the recharge areas of the regional groundwater system is crucial to ensure the safety of the biosphere (Tóth and Sheng, 1996). Furthermore, it can support in identifying the potential migration pathways of radioactive nuclides, forming the foundation for conducting groundwater risk assessments of the site. However, due to the limited number of bedrock groundwater samples obtained in this study, particularly in the eastern of the Beishan area, there is some uncertainty in characterizing the groundwater flow pattern. Additionally, under future extreme events, such as extreme climatic conditions, tectonic movement, and human activities, regional groundwater flow patterns may differ significantly from the current assessment. For the safeguarding of the ecological environment, greater attention should be given to the sustainable exploitation of water resources. Considering the exploitation of groundwater resources, a vital finding is the significantly restricted potential for groundwater resource extraction within the Beishan area. However, this limitation offers an opportunity that can be harnessed for advantageous purposes. Specifically, it presents a favourable context for the secure disposal of HLW and the effective containment of radionuclide dispersion. In this regard, the geological and hydrogeological conditions of the Beishan area provide a strategic advantage for waste management and environmental safeguarding.

5. Conclusions

In this study, we conducted a comprehensive multi-isotope analysis of groundwater circulation in the Beishan, a priority area for China's HLW repositories. Through the integration of D and ^{18}O stable isotopes alongside noble gas isotopes, as well as the insights from ^{3}H and ^{14}C radioactive isotopes, we successfully delineated groundwater recharge sources and quantified groundwater age and renewal rate. Several important conclusions are summarized as follows:

(1) The main sources of shallow groundwater in the Beishan area were local precipitation infiltration, which primarily occurred during the summer recharge period. The mean δD and δ^{18}O values of deep bedrock groundwater showed a statistically significant reduction compared to shallow groundwater. Deep bedrock groundwater was mainly recharged through the infiltration of ancient precipitation under cold climate conditions and has not undergone deep cycling processes.
(2) The ^{3}H content of groundwater in loose sediments was mostly $>$ 10 TU and showed little regularity with depth. In contrast, the bedrock groundwater was mostly $<$ 3.2 TU. For bedrock groundwater at depths over than 70 m, the ^{3}H content was below the detection limit, indicating that the deep bedrock groundwater was primarily recharged by non-modern water.
(3) The groundwater in the gully and piedmont slope loose deposits within the recharge area exhibited significantly younger ages, generally $<$ 30 years. In contrast, the loose sedimentary groundwater age in the intermountain basins and depressions within the discharge area was typically $>$ 50 years. Furthermore, the corrected ^{14}C ages of deep groundwater is generally $>$ 10 ka within the recharge area, indicating the groundwater movement and alteration were extremely slow.
(4) The geographical distributions of shallow groundwater age and annual renewal rate were generally compatible. The annual renewal rate of shallow groundwater in the gully and piedmont slope loose deposits within the recharge area was relatively high (often 5 %–35 %), contrasting with intermountain basins and depressions within the discharge area where it was minimal (usually 0.5 %–1.5 %). Additionally, the annual renewal rate of most shallow bedrock groundwater was $<$ 0.1 %.

In summary, the groundwater source in the Beishan area exhibits distinct characteristics, with deep groundwater displaying remarkably low age and annual renewal rates. This suggests that the movement and alteration of deep groundwater in the Beishan area are exceptionally slow, which is advantageous in constraining the migration of radioactive nuclides. Consequently, the hydrogeological conditions in the Beishan preselected area are conducive to the geological disposal of high-level radioactive waste (HLW). While this study has shed light on the hydrogeological characteristics of deep groundwater, the comprehensive determination of the spatial distribution of deep groundwater age was limited due to data constraints. Therefore, future research should focus on exploring the characteristics of deep groundwater circulation. The construction of the Beishan Underground Research Laboratory (URL), including the excavation of ramps and shafts, has made it more feasible to obtain deep groundwater samples at the site. This presents an opportunity to gather more reliable data and address the limitations of this study.

CRediT authorship contribution statement

Jiebiao Li: Conceptualization, Methodology, Writing – original draft. **You-Kuan Zhang:** Methodology, Writing – review & editing. **Zhichao Zhou:** Conceptualization, Methodology, Writing – review & editing. **Yonghai Guo:** Methodology. **Jingbo Zhao:** Methodology. **Xiuyu Liang:** Conceptualization, Methodology, Writing – review & editing, Supervision.

Declaration of competing interest

The authors declare that they have no known competing financial interests or personal relationships that could have appeared to influence the work reported in this paper.

Data availability

Data will be made available on request.

Acknowledgments

This study was financially supported by the Special Project for Decommissioning of Nuclear Facilities and Radioactive Waste Treatment, which was funded by the State Administration of Science, Technology and Industry for National Defense (Grant Number 2022 [736]), the China National Nuclear Corporation Fundamental Research Project (No. JCYJ2201), the CAEA Innovation Center for Geological Disposal of High-Level Radioactive Wate Foundation (No. CXJJ21102201), the Shenzhen Natural Science Foundation Project (Grant Number JCYJ20190809142203633), the National Natural Science Foundation of China (41977165, 42172275), and Guangdong Provincial Key Laboratory of Soil and Groundwater Pollution Control (No. 2023B1212060002). We thank everyone that contributed to the project, including Ju Wang, Rui Su, Liang Chen, Ruili Ji, Ming Zhang, Yanan Li, Zijian Ji, Xinyu Fu, and Hengrui Chen, among others.

Data availability statement

Data supporting the findings of this study are available from the corresponding author upon request.

Appendix A. Supplementary data

Supplementary data to this article can be found online at https://doi.org/10.1016/j.jhydrol.2023.130592.

References

Apted, M.J., Ahn, J., 2017. Geological repository systems for safe disposal of spent nuclear fuels and radioactive waste, second ed. Woodhead Publishing, pp. xix–xx. https://doi.org/10.1016/B978-0-08-100642-9.05001-5.

Ayraud, V., Aquilina, L., Labasque, T., Pauwels, H., Molenat, J., Pierson-Wickmann, A.-C., Durand, V., Bour, O., Tarits, C., Le Corre, P., Fourre, E., Merot, P., Davy, P., 2008. Compartmentalization of physical and chemical properties in hard-rock aquifers deduced from chemical and groundwater age analyses. Appl. Geochem. 23 (9), 2686–2707. https://doi.org/10.1016/j.apgeochem.2008.06.001.

Barbieri, M., Boschetti, T., Petitta, M., Tallini, M., 2005. Stable isotope (^{2}H, ^{18}O and ^{87}Sr/^{86}Sr) and hydrochemistry monitoring for groundwater hydrodynamics analysis in a karst aquifer (Gran Sasso, Central Italy). Appl. Geochem. 20 (11), 2063–2081. https://doi.org/10.1016/j.apgeochem.2005.07.008.

Batlle-Aguilar, J., Banks, E.W., Batelaan, O., Kipfer, R., Brennwald, M.S., Cook, P.G., 2017. Groundwater residence time and aquifer recharge in multilayered, semi-confined and faulted aquifer systems using environmental tracers. J. Hydrol. 546, 150–165. https://doi.org/10.1016/j.jhydrol.2016.12.036.

Bockgård, N., Rodhe, A., Olsson, K.A., 2004. Accuracy of CFC groundwater dating in a crystalline bedrock aquifer: Data from a site in southern Sweden. Hydrgeol. J. 12 (2), 171–183. https://doi.org/10.1007/s10040-004-0319-3.

Böhlke, J.K., 2006. Tracermodel 1 - Excel workbook for calculation and presentation of environmental tracer data for simple groundwater mixtures: Use of chlorofluorocarbons in hydrology - a guidebook. Section 10 (3).

Cartwright, I., Cendón, D., Currell, M., Meredith, K., 2017. A review of radioactive isotopes and other residence time tracers in understanding groundwater recharge: Possibilities, challenges, and limitations. J. Hydrol. 555, 797–811. https://doi.org/10.1016/j.jhydrol.2017.10.053.

Celle-Jeanton, H., Gourcy, L., Aggarwal, P.K., 2002. Reconstruction of tritium time series in precipitation, International Atomic Energy Agency (IAEA), pp. 430-432.

Chapman, N., Hooper, A., 2012. The disposal of radioactive wastes underground. Proc. Geol. Assoc. 123 (1), 46–63. https://doi.org/10.1016/j.pgeola.2011.10.001.

Chatterjee, S., Sinha, U.K., Ansari, M.A., Mohokar, H.V., Dash, A., 2018. Application of lumped parameter model to estimate mean transit time (MTT) of the thermal water using environmental tracer (3H): Insight from uttarakhand geothermal area (India). Appl. Geochem. 94, 1–10. https://doi.org/10.1016/j.apgeochem.2018.04.013.

Chen, Z., Nie, Z., Zhang, G., Wan, L., Shen, J., 2006. Environmental isotopic study on the recharge and residence time of groundwater in the Heihe River Basin, northwestern China. Hydrgeol. J. 14 (8), 1635–1651. https://doi.org/10.1007/s10040-006-0075-7.

Cheng, Z., Su, C., Zheng, Z., Chen, Z., Wei, W., 2021. Characterize groundwater vulnerability to intensive groundwater exploitation using tritium time-series and hydrochemical data in Shijiazhuang, North China Plain. J. Hydrol. 603 https://doi.org/10.1016/j.jhydrol.2021.126953.

Christofi, C., Bruggeman, A., Kuells, C., Constantinou, C., 2020. Isotope hydrology and hydrogeochemical modeling of Troodos fractured aquifer, Cyprus: The development of hydrogeological descriptions of observed water types. Appl. Geochem. 123 https://doi.org/10.1016/j.apgeochem.2020.104780.

Clark, Fritz, P., 1997. Environmental isotopes in hydrogeology. CRC Press, Boca Raton.

Clauer, N., Frape, S.K., Fritz, B., 1989. Calcite veins of the Stripa granite (Sweden) as records of the origin of the groundwaters and their interactions with the granitic body. Geochim. Cosmochim. Acta 53 (8), 1777–1781. https://doi.org/10.1016/0016-7037(89)90298-6.

Cook, P.G., Love, A.J., Robinson, N.I., Simmons, C.T., 2005. Groundwater ages in fractured rock aquifers. J. Hydrol. 308 (1), 284–301. https://doi.org/10.1016/j.jhydrol.2004.11.005.

Craig, H., 1961. Isotopic variations in meteoric waters. Science 133 (3465), 1702–1703. https://doi.org/10.1126/science.133.3465.1702.

Doney, S.C., Glover, D.M., Jenkins, W.J., 1992. A model function of the global bomb tritium distribution in precipitation, 1960–1986. J. Geophys. Res. Oceans 97 (C4), 5481–5492. https://doi.org/10.1029/92jc00015.

Eriksson, E., 1971. Compartment models and reservoir theory. Annu. Rev. Ecol. Syst. 2 (1), 67–84. https://doi.org/10.1146/annurev.es.02.110171.000435.

Ferguson, G., Cuthbert, M.O., Befus, K., Gleeson, T., McIntosh, J.C., 2020. Rethinking groundwater age. Nat. Geosci. 13 (9), 592–594. https://doi.org/10.1038/s41561-020-0629-7.

Gascoyne, M., 2004. Hydrogeochemistry, groundwater ages and sources of salts in a granitic batholith on the Canadian Shield, southeastern Manitoba. Appl. Geochem. 19 (4), 519–560. https://doi.org/10.1016/S0883-2927(03)00155-0.

Gimeno, M.J., Tullborg, E.-L., Nilsson, A.-C., Auqué, L.F., Nilsson, L., 2023. Hydrogeochemical characterisation of the groundwater in the crystalline basement of Forsmark, the selected area for the geological nuclear repositories in Sweden. J. Hydrol. 624, 129818 https://doi.org/10.1016/j.jhydrol.2023.129818.

Guan, B., 1986. Calculation of tritium of precipitation of China. Hydrogeol. Eng. Geol. 13 (4), 38–41 (in Chinese).

Gumm, L.P., Bense, V.F., Dennis, P.F., Hiscock, K.M., Cremer, N., Simon, S., 2015. Dissolved noble gases and stable isotopes as tracers of preferential fluid flow along faults in the Lower Rhine Embayment, Germany. Hydrogeol. J. 24 (1), 99–108. https://doi.org/10.1007/s10040-015-1321-7.

Guo, X., Feng, Q., Wei, Y., Li, Z., Liu, W., 2015. An overview of precipitation isotopes over the Extensive Hexi Region in NW China. Arab. J. Geosci. 8 (7), 4365–4378. https://doi.org/10.1007/s12517-014-1521-9.

Guo, Y., Wang, H., Dong, J., Su, R., Liu, S., Zhou, Z., 2013. Isotopic study of deep groundwater in Jijicao preselected site for China's high level radioactive waste disposal repository. Acta Geol. Sin. 87 (9), 1477–1485 (in Chinese).

Gupta, H.V., Kling, H., Yilmaz, K.K., Martinez, G.F., 2009. Decomposition of the mean squared error and NSE performance criteria: Implications for improving hydrological modelling. J. Hydrol. 377 (1), 80–91. https://doi.org/10.1016/j.jhydrol.2009.08.003.

Han, L.-F., Plummer, L.N., Aggarwal, P., 2012. A graphical method to evaluate predominant geochemical processes occurring in groundwater systems for radiocarbon dating. Chem. Geol. 318–319, 88–112. https://doi.org/10.1016/j.chemgeo.2012.05.004.

Han, L.F., Plummer, L.N., 2016. A review of single-sample-based models and other approaches for radiocarbon dating of dissolved inorganic carbon in groundwater. Earth Sci. Rev. 152, 119–142. https://doi.org/10.1016/j.earscirev.2015.11.004.

He, J., Ma, J., Zhang, P., Tian, L., Zhu, G., Mike Edmunds, W., Zhang, Q., 2012. Groundwater recharge environments and hydrogeochemical evolution in the Jiuquan Basin, Northwest China. Appl. Geochem. 27 (4), 866–878. https://doi.org/10.1016/j.apgeochem.2012.01.014.

IAEA, 1989. Safety principles and technical criteria for the underground disposal of high level radioactive wastes. International Atomic Energy Agency, Vienna.

Jasechko, S., 2019. Global isotope hydrogeology-review. Rev. Geophys. 57 (3), 835–965. https://doi.org/10.1029/2018rg000627.

Joshi, S.K., Rai, S.P., Sinha, R., Gupta, S., Densmore, A.L., Rawat, Y.S., Shekhar, S., 2018. Tracing groundwater recharge sources in the northwestern Indian alluvial aquifer using water isotopes (δ^{18}O, δ^{2}H and ^{3}H). J. Hydrol. 559, 835–847. https://doi.org/10.1016/j.jhydrol.2018.02.056.

Jr, F.J.P., Balderer, W., Loosli, H.H., Lehmann, B.E., Matter, A., Peters, T., Schmassmann, H., Gautschi, A., 1991. Applied isotope hydrogeology: a case study in Northern Switzerland. In: Gautschi, A. et al. (Eds.), Studies in Environmental Science. Elsevier, pp. 175-237. 10.1016/S0166-1116(08)70497-7.

Jurgens, B.C., Böhlke, J.K., Eberts, S.M., 2012. TracerLPM (Version 1): An Excel® workbook for interpreting groundwater age distributions from environmental tracer data. 4-F3, Reston, VA. DOI:10.3133/tm4F3.

Kagabu, M., Matsunaga, M., Ide, K., Momoshima, N., Shimada, J., 2017. Groundwater age determination using ^{85}Kr and multiple age tracers (SF6, CFCs, and ^{3}H) to elucidate regional groundwater flow systems. J. Hydrol.: Reg. Stud. 12, 165–180. https://doi.org/10.1016/j.ejrh.2017.05.003.

Kamtchueng, B.T., Fantong, W.Y., Wirmvem, M.J., Tiodjio, R.E., Takounjou, A.F., Asai, K., Djomou, S.L.B., Kusakabe, M., Ohba, T., Tanyileke, G., Hell, J.V., Ueda, A., 2015. A multi-tracer approach for assessing the origin, apparent age and recharge mechanism of shallow groundwater in the Lake Nyos catchment, Northwest, Cameroon. J. Hydrol. 523, 790–803. https://doi.org/10.1016/j.jhydrol.2015.02.008.

La Salle, C.L., Marlin, C., Leduc, C., Taupin, J.D., Massault, M., Favreau, G., 2001. Renewal rate estimation of groundwater based on radioactive tracers (H-3, C-14) in an unconfined aquifer in a semi-arid area, Iullemeden Basin, Niger. J. Hydrol. 254 (1–4), 145–156. https://doi.org/10.1016/S0022-1694(01)00491-7.

Laaksoharju, M., Gascoyne, M., Gurban, I., 2008a. Understanding groundwater chemistry using mixing models. Appl. Geochem. 23 (7), 1921–1940. https://doi.org/10.1016/j.apgeochem.2008.02.018.

Laaksoharju, M., Smellie, J., Tullborg, E.-L., Gimeno, M., Molinero, J., Gurban, I., Hallbeck, L., 2008b. Hydrogeochemical evaluation and modelling performed within

the Swedish site investigation programme. Appl. Geochem. 23 (7), 1761–1795. https://doi.org/10.1016/j.apgeochem.2008.02.015.
Li, Z., Si, B., 2018. Reconstructed precipitation tritium leads to overestimated groundwater recharge. J. Geophys. Res. Atmos. 123 (17), 9858–9867. https://doi.org/10.1029/2018jd028405.
Li, J., Su, R., Zhou, Z., Guo, Y., 2020a. Hydrochemical and stable isotope characteristics of precipitation in Beishan Area. China Environ. Sci. 40 (12), 5152–5161 (in Chinese).
Li, M., Xin, H., Tian, J., Meng, X., Pang, Z., Chen, C., Liang, G., 2020b. Composition, Age and Polarity of Gongpoquan Arc and Its Tectonic Significance in Beishan Orogen. Earth Sci. 45 (7), 2393–2412 (in Chinese).
Li, J., Zhou, Z., Yun, L., Su, R., Guo, Y., 2022. Identification of hidden faults based on soil radon measurement in the southern margin of the Beishan area, Gansu Province. Acta Geol. Sinica 96 (6), 2240–2250 (in Chinese).
Liu, J., Chen, Z., Wei, W., Zhang, Y., Li, Z., Liu, F., Guo, H., 2014. Using chlorofluorocarbons (CFCs) and tritium (^{3}H) to estimate groundwater age and flow velocity in Hohhot Basin, China. Hydrol. Process. 28 (3), 1372–1382. https://doi.org/10.1002/hyp.9659.
Lu, Z.T., Schlosser, P., Smethie, W.M., Sturchio, N.C., Fischer, T.P., Kennedy, B.M., Purtschert, R., Severinghaus, J.P., Solomon, D.K., Tanhua, T., Yokochi, R., 2014. Tracer applications of noble gas radionuclides in the geosciences. Earth Sci. Rev. 138, 196–214. https://doi.org/10.1016/j.earscirev.2013.09.002.
Lucas, L.L., Unterweger, M.P., 2000. Comprehensive review and critical evaluation of the half-life of tritium. J. Res. Nat. Inst. Stand. Technol. 105 (4), 541–549. https://doi.org/10.6028/jres.105.043.
Ma, B., Jin, M., Liang, X., Li, J., 2019. Application of environmental tracers for investigation of groundwater mean residence time and aquifer recharge in fault-influenced hydraulic drop alluvium aquifers. Hydrol. Earth Syst. Sci. 23 (1), 427–446. https://doi.org/10.5194/hess-23-427-2019.
Maloszewski, P., Zuber, A., 1996. Lumped parameter models for the interpretation of environmental tracer data. International Atomic Energy Agency, Vienna (Austria), IAEA. Journal, ID.
Małoszewski, P., Zuber, A., 1982. Determining the turnover time of groundwater systems with the aid of environmental tracers: 1. Models and their applicability. J. Hydrol. 57 (3), 207–231. https://doi.org/10.1016/0022-1694(82)90147-0.
Morgenstern, U., Taylor, C.B., 2009. Ultra low-level tritium measurement using electrolytic enrichment and LSC. Isot. Environ. Health Stud. 45 (2), 96–117. https://doi.org/10.1080/10256010902931194.
Münnich, K.O., 1957. Messungen des C14-Gehaltes von hartem Grundwasser. Naturwissenschaften. 44 (2), 32–33. https://doi.org/10.1007/BF01146093.
Nilsson, A.-C., Gimeno, M.J., Tullborg, E.-L., Smellie, J., Jönsson, S., Puigdomenech, I., Berg, C., 2020. Methodology for hydrogeochemical sampling to characterise groundwaters in crystalline bedrock: developments made within the Swedish radwaste programme. Geofluids 2020, 8740492. https://doi.org/10.1155/2020/8740492.
Niu, Y., Castro, M.C., Hall, C.M., Gingerich, S.B., Scholl, M.A., Warrier, R.B., 2017. Noble gas signatures in the Island of Maui, Hawaii: Characterizing groundwater sources in fractured systems. Water Resour. Res. 53 (5), 3599–3614. https://doi.org/10.1002/2016WR020172.
Ozyurt, N.N., Bayari, C.S., 2003. LUMPED: a Visual Basic code of lumped-parameter models for mean residence time analyses of groundwater systems. Comput. Geosci. 29 (1), 79–90. https://doi.org/10.1016/S0098-3004(02)00075-4.
Pang, Z., Kong, Y., Li, J., Tian, J., 2017. An isotopic geoindicator in the hydrological cycle. Procedia Earth Planet. Sci. 17, 534–537. https://doi.org/10.1016/j.proeps.2016.12.135.
Pitkaenen, P., Partamies, S., Luukkonen, A., 2004. Hydrogeochemical interpretation of baseline groundwater conditions at the Olkiluoto site, Posiva Oy, Helsinki (Finland), Finland.
Priebe, E.H., Frape, S.K., Jackson, R.E., Rudolph, D.L., Brunton, F.R., 2021. Tracing recharge and groundwater evolution in a glaciated, regional-scale carbonate bedrock aquifer system, southern Ontario, Canada. Appl. Geochem. 124 https://doi.org/10.1016/j.apgeochem.2020.104794.
Putman, A.L., Fiorella, R.P., Bowen, G.J., Cai, Z., 2019. A Global Perspective on Local Meteoric Water Lines: Meta-analytic Insight Into Fundamental Controls and Practical Constraints. Water Resour. Res. 55 (8), 6896–6910. https://doi.org/10.1029/2019WR025181.
Sano, Y., Wakita, H., 1985. Geographical distribution of ^{3}He/^{4}He ratios in Japan: Implications for arc tectonics and incipient magmatism. J. Geophys. Res. Solid Earth. 90 (B10), 8729–8741. https://doi.org/10.1029/JB090iB10p08729.
Siegenthaler, U., Oeschger, H., 1980. Correlation of ^{18}O in precipitation with temperature and altitude. Nature. 285 (5763), 314–317. https://doi.org/10.1038/285314a0.
Tian, J., Pang, Z., Liao, D., Zhou, X., 2021. Fluid geochemistry and its implications on the role of deep faults in the genesis of high temperature systems in the eastern edge of the Qinghai Tibet Plateau. Appl. Geochem. 131, 105036 https://doi.org/10.1016/j.apgeochem.2021.105036.
Tomonaga, Y., Marzocchi, R., Pera, S., Pfeifer, H.-R., Kipfer, R., Decrouy, L., Vennemann, T., 2017. Using noble-gas and stable-isotope data to determine groundwater origin and flow regimes: Application to the Ceneri Base Tunnel (Switzerland). J. Hydrol. 545, 395–409. https://doi.org/10.1016/j.jhydrol.2016.11.043.
Tóth, J., Sheng, G., 1996. Enhancing safety of nuclear waste disposal by exploiting regional groundwater flow: the recharge area concept. Hydrgeol. J. 4 (4), 4–25. https://doi.org/10.1007/s100400050252.
Tsang, C.-F., Neretnieks, I., Tsang, Y., 2015. Hydrologic issues associated with nuclear waste repositories. Water Resour. Res. 51 (9), 6923–6972. https://doi.org/10.1002/2015wr017641.
Wang, J., Chen, W., Su, R., Guo, Y., Jin, Y., 2006. Geological disposal of high-level radioactive waste and its key scientific issues. Chin. J. Rock Mech. Eng. 25 (4), 801–812 (in Chinese).
Wang, J., Chen, L., Su, R., Zhao, X., 2018. The Beishan underground research laboratory for geological disposal of high-level radioactive waste in China: Planning, site selection, site characterization and in situ tests. J. Rock Mechan. Geotechn. Eng. 10 (3), 411–435. https://doi.org/10.1016/j.jrmge.2018.03.002.
Warr, O., Sherwood Lollar, B., Fellowes, J., Sutcliffe, C.N., McDermott, J.M., Holland, G., Mabry, J.C., Ballentine, C.J., 2018. Tracing ancient hydrogeological fracture network age and compartmentalisation using noble gases. Geochim. Cosmochim. Acta. 222, 340–362. https://doi.org/10.1016/j.gca.2017.10.022.
Watson, G.S., 1971. Trend-surface analysis. J. Int. Assoc. Math. Geol. 3 (3), 215–226. https://doi.org/10.1007/BF02045792.
Wurster, C.M., Patterson, W.P., McFarlane, D.A., Wassenaar, L.I., Hobson, K.A., Athfield, N.B., Bird, M.I., 2008. Stable carbon and hydrogen isotopes from bat guano in the Grand Canyon, USA, reveal Younger Dryas and 8.2 ka events. Geol. 36 (9), 683–686. https://doi.org/10.1130/g24938a.1.
Yun, L., Zhang, J., Wang, J., Yang, X., Qu, J., Zhang, B., Zhao, H., 2020. Active deformation to the north of the Altyn Tagh Fault: Constraints on the northward growth of the northern Tibetan Plateau. J. Asian Earth Sci. 198 https://doi.org/10.1016/j.jseaes.2020.104312.
Zhai, Y., Wang, J., Guo, H., Cao, Y., Teng, Y., 2013. Reconstruction and optimization of tritium time series in precipitation of Beijing, China. Radiocarbon 55 (1), 67–79. https://doi.org/10.2458/azu_js_rc.v55i1.16043.
Zhang, J., Wang, X.-S., Yin, L., Wang, W., Love, A., Lu, Z.-T., Jiang, W., Yang, G.-M., Xie, Y., Wang, X., Sun, F., Tang, X., Hou, G., Pang, Z., 2021. Inflection points on groundwater age and geochemical profiles along wellbores light up hierarchically nested flow systems. Geophys. Res. Lett. 48 (16) https://doi.org/10.1029/2020GL092337 e2020GL092337.
Zhong, C., Yang, Q., Ma, H., Bian, J., Zhang, S., Lu, X., 2019. Application of environmental isotopes to identify recharge source, age, and renewability of phreatic water in Yinchuan Basin. Hydrol. Process. https://doi.org/10.1002/hyp.13468.
Zhou, Z., Wang, J., Su, R., Guo, Y., Zhao, J., Zhang, M., Ji, R., Li, Y., Li, J., 2020. Hydrogeochemical and isotopic characteristics of groundwater in Xinchang preselected site and their implications. Environ. Sci. Pollut. Res. 27 (28), 34734–34745. https://doi.org/10.1007/s11356-019-07208-1.
Zhou, Z., Wang, J., Su, R., Guo, Y., Li, J., Zhao, J., Zhang, M., Ji, R., Li, Y., 2022. Formation mechanism of deep groundwater at the Xinchang site of high-level radioactive waste geological disposal in China. J. Radioanal. Nucl. Chem. https://doi.org/10.1007/s10967-022-08697-0.
Zongyu, C., Jixiang, Q., Jianming, X., Jiaming, X., Hao, Y., Yunju, N., 2003. Paleoclimatic interpretation of the past 30 ka from isotopic studies of the deep confined aquifer of the North China plain. Appl. Geochem. 18 (7), 997–1009. https://doi.org/10.1016/S0883-2927(02)00206-8.
Vogel, J.C., 1967. Investigation of groundwater flow with radiocarbon: Isotopes in Hydrology, Proceedings from Conference on Isotopes in Hydrology, Int. Atomic Energy Agency, Vienna, pp. 355-368.